On the Dependence between FPC and ICIC in SC-FDMA Cellular Systems

Javier Lafuente-Martínez [1], Ángela Hernández-Solana [2], Antonio Valdovinos [3]
Aragon Institute for Engineering Research (I3A), University of Zaragoza, 50018 Zaragoza (Spain)
{[1]javierlm, [2]anhersol, [3]toni}@unizar.es

Abstract—**The performance of an SC-FDMA cellular system highly depends on the proper selection of the parameters involved in the Fractional Power Control (FPC) algorithm. When a real cellular system is deployed, a power control algorithm must be combined with a resource allocation strategy under some interference coordination scheme, such as the well known Fractional Frequency Reuse (FFR). However, in order to set a suitable operation point for FPC, previous studies have not considered enough the joint behavior of all those factors. In this paper, we analyze how the system performance is affected when different FPC operation points are combined with different Inter-Cell or Inter-Sector Interference Coordination (ICIC/ISIC) schemes derived from FFR. Our study reveals that different power control parameters must be set depending on the per-cell or per-sector basis of the frequency reuse strategy considered in the interference coordination scheme.**

Keywords: FFR, FPC, ICIC, ISIC, SC-FDMA, Uplink.

I. INTRODUCTION

The Single Carrier Frequency Division Multiple Access Scheme (SC-FDMA) is a well-known modified form of OFDMA that has been selected by the 3GPP as the uplink (UL) multiple access scheme for Long Term Evolution (LTE) [1]. This scheme allows reducing the Power Average Peak Ratio (PAPR) in UL transmissions, which greatly benefits the mobile terminals in terms of transmitted power efficiency. Also, thanks to the orthogonal nature of its carriers, it prevents the system from intra-cell interference. However, in order to cope with the increasing demand of capacity, it is common to reuse the same frequency resources within all the cells/sectors in a cellular system, thus causing the problem of Inter-Cell Interference (ICI) and Inter-Sector Interference (ISI). Therefore, some ICI/ISI management strategy, i.e. a combination of power control (PC) and resource allocation (RA) under some ICI/ISI Coordination (ICIC/ISIC) scheme, becomes necessary.

In this sense, Fractional Frequency Reuse (FFR), which aims to reduce the ICI by providing orthogonal frequency resources to cell-edge users, has been widely proposed [2-4], but the authors usually do not consider the joint behavior of ICIC and power control. Also, the Fractional Power Control (FPC) algorithm has been established as a standard for the UL in LTE [5]. Since FPC was standardized, different studies have discussed about the proper values for both its open-loop and close-loop parameters [6-8], but the authors usually do not consider any specific ICIC/ISIC scheme in their simulations.

The idea of increasing the spectral efficiency by reusing frequency resources on a per-sector basis has also been suggested, but mainly for the downlink (DL) [9,10]. This deployment, which naturally increases the number of users that can be served per Transmission Time Interval (TTI) at the expense of generating ISI, was recently analyzed for the UL in [11] where we proposed some novel FFR-based ICIC/ISIC schemes that proved to be efficient for reducing the ICI/ISI and for increasing the capacity of SC-FDMA cellular systems.

In this work, we analyze the joint behavior of FPC and different FFR-based ICIC/ISIC schemes. We determine that, in order to increase the cellular system performance, a different FPC operation point must be selected depending on the per-cell or per-sector basis of the frequency reuse strategy being considered. Furthermore, we will recommend some specific values for the open-loop parameters of FPC.

The rest of the paper is organized as follows: Section II shows the system model framework. The ICIC/ISIC schemes considered in the cellular system are described in section III. The simulation methodology, operating conditions and performance analysis are included in section IV. Conclusions are finally drawn in section V.

II. SYSTEM MODEL FRAMEWORK

We consider the UL of an LTE multi-cell system, in which each cell independently performs its scheduling decisions at each TTI taking into account the constraints imposed by the ICIC/ISIC schemes.

Each cell consists of three sectors. In order to get more control over the resource allocation strategy and over the simulation results, we have divided the cell range into three concentric same-area virtual zones (Fig.1-a). This allows us to define cell-center (UE_{cc}) and cell-edge users (UE_{ce}) by comparing their mean channel-loss with the distance-loss corresponding to the frontier between virtual zones 1 and 2. As we consider a channel-loss criterion, users are classified taking into account not only the distance to their Base Station (BS), but also the sector antenna patterns and the shadowing effects.

In addition, to cope with the particularities of some ISIC schemes, we have defined three *frontier areas* which extend at both sides of the frontier between sectors (Fig.1-b). Users belonging to these areas are called *frontier users* (UE_{fr}).

978-1-4673-1881-5/12/$31.00 ©2012 IEEE

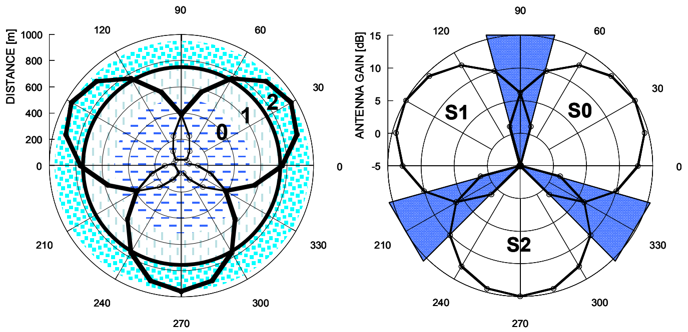

Figure 1. a) Virtual zones vs channel-loss b) Antenna pattern

RA has been considered as a multidimensional assignment problem: an FFR-based ICIC/ISIC scheme determines the sets of frequency resources that should be preferably assigned for each cell/sector or for each cell-edge/cell-center virtual zone, whereas the packet scheduling (PS) determines which of the available resources are allocated to the schedulable users. PS is divided into two steps. First, a time-domain (TD) scheduling determines the priority order of the schedulable users at each TTI according to some QoS metric. Then, a frequency domain (FD) scheduling determines the PRB, the power and the data rate to be allocated for each user.

In this study, we consider that users transmit real-time traffic with hard delay requirements. Packets exceeding a maximum packet-delay constraint are dropped. In those conditions, the overall system capacity can be evaluated in terms of the number of users supported while satisfying a specific packet dropping mean threshold (1%). In order to deal with these hard-delay requirements, we consider the *Modified Largest Delay First* (*M-LDF*) TD metric (1), calculated as the ratio of the delay of the first packet in the buffer of user k ($W_k[n]$) in the n-th TTI, to the maximum packet delay $d_{max,k}$:

$$k^* = \arg\max_k \left\{ W_k[\mathrm{n}] / d_{\max,k} \right\} \qquad (1)$$

From the FD scheduling perspective, a channel-dependent RA is considered, that is, frequency resources are assigned according to the Channel to Interference and Noise Ratio (CINR) that users are expected to experience on them. A detailed description of the RA algorithms is given section III.

Following the LTE recommendations, system frequency resources are divided into N_{PRB} Physical Resource Blocks (PRBs), which is the minimum allocable resource unit. A PRB comprises N_{SC} subcarriers for N_T consecutive OFDM symbols (data symbols of one subframe/TTI), and the same transmitted power and Modulation and Coding Scheme (MCS) are applied to all the subcarriers within a PRB. Transmission power for the Physical Uplink Shared CHannel (PUSCH) is determined by means of the standard open-loop FPC algorithm. We consider that scheduled users are assigned a single PRB, which yields to the simplified formula (2).

$$P_{PUSCH} = \min\left\{ P_{MAX}, P_{O\_PUSCH} + \alpha PL \right\} \qquad (2)$$

P_{MAX} is the maximum user transmission power, α is a cell specific path-loss compensation factor and PL is the UL path-loss. P_{O_PUSCH} (3) is a user-and-cell-dependent parameter computed so that a user transmitting P_{MAX} can reach a mean SINR value ($SINR_{OBJ}$) at a particular distance from its Base Station (BS) and assuming a mean Interference over Thermal noise on the whole scenario (IoT_{OBJ}) [11]. Thus, the operation point for the power control algorithm depends on these three parameters: $SINR_{OBJ}$, IoT_{OBJ} and α, and must be carefully set to allow users placed at the beginning of the external virtual zone to transmit all the data generated at each TTI on a single PRB, using a defined MCS.

$$P_{O\_PUSCH} = (1-\alpha)P_{\max}^{RB} + \alpha(SINR_{OBJ} + IoT_{OBJ} + N) \qquad (3)$$

In order to improve the system performance, Adaptive MCS (AMCS) is implemented to adapt data transmissions according to the SINR expected on the PRBs assigned to each user. Thus, cell-edge users will usually get a lower SINR and will be assigned a lower MCS, whilst users near the BS could use a higher MCS to transmit in case of having remaining traffic. We do not consider any delay on power and scheduling decisions and we assume a perfect knowledge of the channel by the BS, although the expected interference is estimated from previous transmissions in order to compute the CINR and thus the Signal to Interference and Noise Ratio (SINR).

III. RESOURCE ALLOCATION SCHEMES

Our aim is to evaluate the joint behavior power control and resource allocation under different ICIC/ISIC schemes. For this purpose, we have considered three representative interference coordination schemes which have proven to enhance the performance of the traditional FFR1/3 for SC-FDMA cellular systems. In this section we give an outline of the schemes. Further details of their algorithms, previously proposed by these authors, are explained in [12]. All the schemes are jointly represented in Fig.2. Note that, in this figure, the PRBs depicted on each sector/zone of the cell should be considered as the first choice for users belonging to that sector/zone, but those PRBs can be finally assigned to users belonging to another sector/zone. Thus, we are considering *soft-FFR* schemes. Also, the PRBs depicted on the *frontier areas* must be considered as belonging to the inner subband for those schemes that do not consider *frontier users*.

A. FFR 1/3 with sector-and-zone coordination (FFR1/3_sz)

The first scheme reuses frequency resources only once per cell. In order to compute the first allocation trial for each user, we pre-allocate orthogonal PRBs not only for UE_{ce} as traditional FFR1/3 schemes, but also for UE_{cc}. Then, those PRBs are coordinated within each sector and virtual zone in the cell, and also among neighbouring cells as depicted in Fig.2. The available spectrum is split into a reuse-1 inner subband, intended for UE_{cc}, and a reuse-1/3 outer subband in which UE_{ce} are preferably allocated as a first choice. Resources belonging to the inner subband are further split into three equal-size sector-preferent sets with the aim of grouping users belonging to the same sector, thus reducing the ICI especially in low loaded scenarios. We assume that the outer subband must cover one third of the cell coverage area.

The proposed algorithm follows these steps:

Step 1: Priorize users according to the TD metric. For each user k, try to allocate resources from its preferent set of PRBs depending on the user sector and type (UE_{cc} , UE_{ce}).

Step 2: Select the free PRB from that set in which user k experiences the best CINR, and determine the highest MCS that user k is able to use in it by comparing user's expected SINR with the SINR thresholds considered in the MCS set used for adaptation (see Table I below). In case that even the lowest MCS is not supported, continue with the next step.

Step 3: If user k is unable to find a suitable PRB in its preferred set, or all the PRBs in that set are already assigned to other users, repeat step 2 until a PRB is assigned following this search order:

a) if k is a cell-center user, try *another-sector-preferent* inner set of PRBs. In particular, try first the set with more free resources and then the remaining one. If no suitable PRB is still found, try the set of PRBs from the outer subband corresponding to the sector which user k belongs to.

b) if k is a cell-edge user, try first the set of inner PRBs considered preferent for its sector, then try *another-sector-preferent* inner set (the one with more free resources), and finally the remaining inner set.

Step 4: If no suitable PRB is found, that is, if user k is unable to use at least the lowest MCS in any PRB, it doesn't receive any resources at this TTI.

B. *FFR1/3_sz adapted for reuse-1 per sector (FFR_sz_s)*

In order to increase the system capacity, this scheme proposes to reuse frequency resources on a per-sector basis. In particular, as we consider that cells are divided into three sectors, we allow to assign the PRBs that belong to the inner subband depicted in Fig.2, up to three times within the same cell (reuse-3). Thus, this algorithm differs from FFR1/3_sz in the inner frequency assignments. Now, the PRBs can be allocated to a user k despite they are already assigned to users belonging to a sector different from that of user k.

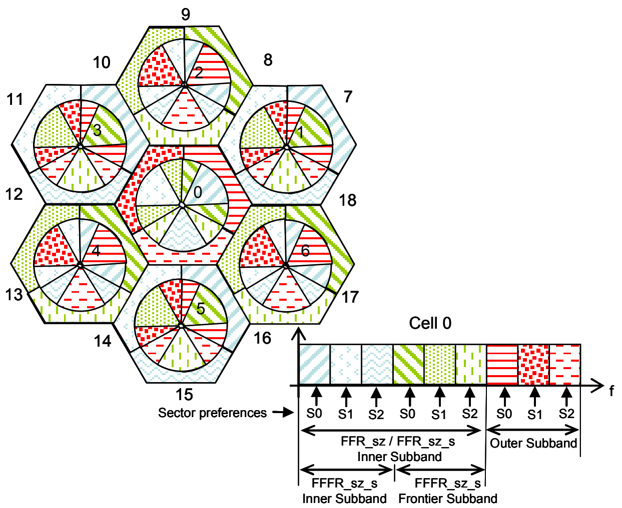

Figure 2. Joint representation of simulated ICIC/ISIC schemes

C. *FFR_sz_s with specific frontier resources (FFFR_sz_s)*

Finally, to compute the first allocation trial for each user in FFFR_sz_s, *frontier areas* are taken into account in order to reduce the ISI. We split the inner subband into two equal-size subbands: a reuse-3 *sector-preferent* subband intended for UE_{cc} and a reuse-3 *frontier-preferent* subband intended for UE_{fr} as depicted in Fig.2. According to this spectrum division, the *frontier areas* extend 30º at both sides of each frontier between sectors, in order to get the same proportion for each type of users in the cell. Frontier users follow a PRB allocation order similar to the one explained for cell-center users in the previous schemes. First, they try to allocate a PRB from the set of *frontier-preferent* PRBs depending on the user's frontier. Then, they try *another-frontier-preferent* set of PRBs taking into account that the selected PRB could be already assigned to users belonging to other sectors, but it cannot be assigned to users belonging to the same *frontier area*. Then, they try to allocate a PRB from their *sector-preferent* inner set depending on the user's sector, and finally, if a suitable PRB is still not found, frontier users try inner sets of PRBs which were initially pre-allocated for other sectors, starting from the one which has less resources assigned to users belonging to the same sector as the frontier user being considered.

IV. SIMULATION RESULTS

A. *Simulation parameters*

The evaluation has been carried out with the set of parameters collected in Table I, following the LTE system level parameters and the FDD frame structure.

TABLE I. SIMULATION PARAMETERS

System Model	
Cell deployment / ISD	21 tri-sectorized cells / 1732m Wrap-around (to avoid border effects)
Carrier frequency	2.5GHz
Path-loss model	$128.1+37.6\log_{10}(d(km))$
Shadowing variance	8dB
Shadowing correlation distance	50m
Shadowing correl. between cells	0.5
Receiver Noise Figure	5dB
System bandwidth / Nr. of PRBs	5MHz / 27 PRBs
PRB size	12 subcarriers for 1 TTI (1 ms)
Channel model (3km/h)	Extended Pedestrian-A
Doppler model	Jakes
BS/UE antenna gain	15dB(BS) / 0dB (UE)
BS antenna horizontal pattern	70deg (-3dB), 20dB front-to-back
TX/RX diversity gain	3dB /3dB
Subframe duration (TTI)	1ms
ARQ delay (Δ_{ARQ})	6ms
Traffic pattern	T_{ON}=30ms, T_{OFF}=90ms dmax=50ms
Power Parameters	
Power control algorithm	Open-loop Fractional Power Control
Maximum output power P_{max}	24dBm
Loss compensation factor α	0.4,0.6,0.8,1.0
$SINR_{OBJ}$/ IoT_{OBJ}	14dB / 10dB,12dB,14dB,16dB

MCS Set Considered						
MCS index	0	1	2	3	4	5
Configuration	QPSK 1/2	QPSK 3/4	16QAM 1/2	16QAM 3/4	64QAM 2/3	64QAM 3/4
Info bits per PRB	120	180	240	360	480	540
SINR threshold	6.2dB	10.0dB	13.5dB	17.4dB	23.4dB	25.5dB

Users move at 3km/h within their respective sector to avoid handovers. The simulation scenario assumes users homogeneously distributed along the coverage area of each cell. The number of active users per cell ranges from 27 to 162 to test different loading scenarios (from 25% to 150%). Data services have been modeled as ON-OFF traffics with an activity factor of 0.25. ON and OFF holding time has been modeled as an exponential random variable with mean T_{ON}=30ms and mean T_{OFF}=90ms, respectively. During the ON state, a new packet of size L=240 bits is generated every TTI. This packet is divided into 4 transport units (TUs), being a TU the minimum data block size that can be transmitted. A maximum delay constraint of d_{max}=50ms is assumed and a hard deadline is applied. The set of MCSs allowed for MCS adaptation is collected also in Table I, along with their minimum SINR threshold (computed to achieve a BLER of 10^{-2}) and their information data rate. An ARQ mechanism based on erroneous block retransmission is also included (assuming a delay of Δ_{ARQ}).

As we explained in section II, the operation point for the power control algorithm depends on these three parameters: $SINR_{OBJ}$, IoT_{OBJ} and α. In order to allow users placed at the frontier between virtual zones 1 and 2 to transmit all the data generated at each TTI on a single PRB, we consider 16QAM½ as the reference modulation and coding scheme, which has a SINR threshold of 13.5dB. Thus, users experiencing a SINR between 13.5dB and 17.4dB will use the reference MCS. Therefore, $SINR_{OBJ}$ must belong to this interval. We consider that it is reasonable to ask users for reaching a $SINR_{OBJ}$ value of 14dB, through the FPC formula (3), as it includes a margin over the SINR threshold of the desired MCS. According to previous studies found in the literature [13], the value of IoT_{OBJ} depends on the cause that limits the range of the cell: in an interference-limited scenario a value of 14dB is suggested, whilst in a noise-limited scenario a value of 2dB is preferred. As we are testing an interference-limited scenario, we have considered IoT_{OBJ}=14dB as a reference value, but we have additionally tested lower and higher values. We also study the impact of different α values in the system performance. According to the FPC formula (2), a decrease in α allows users with the best channel conditions (those with $PL<PL_{zone1\text{-}zone2}$) to increase their transmitted power in order to reach a higher SINR but, in turn, this will increase the mean IoT experienced by other users in the cellular system. We have tested values ranging from 0.4 to 1.0, where 1.0 is considered as full-compensation which means that users try to compensate their whole path loss.

B. Numerical results

Dropping probability has been selected for the evaluation of the cellular system performance, as it is related to the capacity of the system in terms of the number of users that can be supported while guaranteeing an acceptable QoS.

In Fig.3, we show the impact of considering different values for α, in the system performance. For this evaluation, we have considered a $SINR_{OBJ}$=14dB and the reference IoT value (IoT_{OBJ}=14dB) mentioned above. First, we can notice that, when α≥0.6, the methods that reuse frequency resources per sector (Fig.3-b,c) outperform those with reuse-1 per-cell (Fig.3-a). In fact, given a dropping threshold, the number of users supported is increased. This shows that, globally, the negative impact of the inter-sector interference that appears in FFR_sz_s and FFFR_sz_s, is overcome by the benefits of having more available resources to transmit. In general terms, when FPC is considered, i.e. for α values lower than 1, α variation has a similar impact on the proposed schemes: the lower the value of α, the higher the dropping for both the reuse-1 per-cell and per-sector schemes. But if we establish a 1% packet dropping constraint in the system, the best performance is reached with a different value for α, i.e. α=0.6 when reusing frequency resources per cell (Fig.3-a) and α=0.8 if frequency resources are reused per sector (Fig.3-b,c). This behavior can be explained through the FPC formulas (2) and (3): the use of a higher α yields to a decrease in the power transmitted by cell-center users, which in turn reduces the inter-sector interference. In fact, when we compare the system performance in terms of capacity for the best scheme (FFFR_sz_s), if we establish a 1% packet dropping constraint in the system, the amount of users supported per cell is about 10% higher when we consider α=0.8 instead of α=0.6.

Once a suitable value for α is determined, in Fig.4 we evaluate the effect of varying P_0 in the FPC formula (2) by means of increasing or decreasing the value of IoT_{OBJ} in (3). For this evaluation, we consider that a suitable operation point is reached when the expected $SINR_{OBJ}$ and IoT_{OBJ} values match the mean SINR and the mean IoT obtained for the cellular system through the simulations. As the performance of both reuse-1 per-sector schemes (FFR_sz_s and FFFR_sz_s) vary with IoT_{OBJ} in a similar way, we have omitted the FFR_sz_s results in order to show a clearer representation in the figures. Fig.4-a shows how dropping increases when IoT_{OBJ} is increased, due to the corresponding increase in the user's transmitted power. This trend is similar for both the reuse-1 per-cell and per-sector schemes. But, although the system performance seems to be improved by reducing IoT_{OBJ}, our simulations show a button bound for this parameter: results for IoT_{OBJ}=12dB start to outperform those for IoT_{OBJ}=10dB when there is a high load in the system (around 120 users per cell). Also, IoT_{OBJ}=12dB is the value that better match the mean IoT actually obtained for the cellular system in our simulations, as we can see in Fig.4-b for a high-loaded scenario (108 users per cell). We have obtained a mean SINR (Fig.4-c) around 14dB for reuse-1 per-sector schemes, and around 16dB for reuse-1 per-cell schemes, independently of the IoT_{OBJ} being considered.

Our results show that cell-based and sector-based interference coordination schemes respond to IoT_{OBJ} variations in a similar way (Fig.4), but their behavior is slightly different when varying α (Fig.3). The suitable operation point that should be considered in the FPC formula is therefore different when implementing ICIC/ISIC schemes with frequency reuse-1 per-cell ($SINR_{OBJ}$=14dB, IoT_{OBJ}=12dB, α=0.6) or frequency reuse-1 per-sector ($SINR_{OBJ}$=14dB, IoT_{OBJ}=12dB, α=0.8).

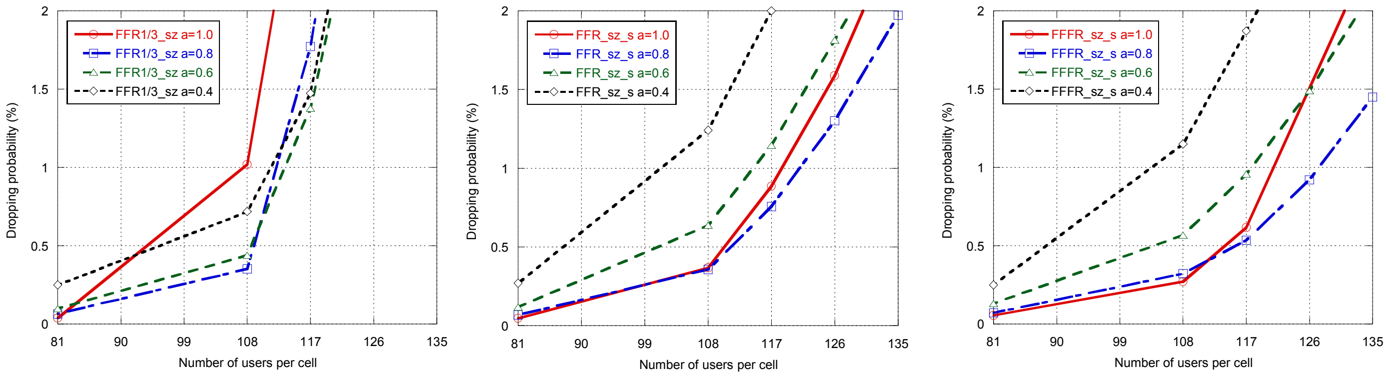

a) Dropping Probability – FFR1/3_sz b) Dropping Probability – FFR_sz_s c) Dropping Probability – FFFR_sz_s

Figure 3. Dependence of the system performance with α ($SINR_{OBJ}$=14dB, IoT_{OBJ}=14dB)

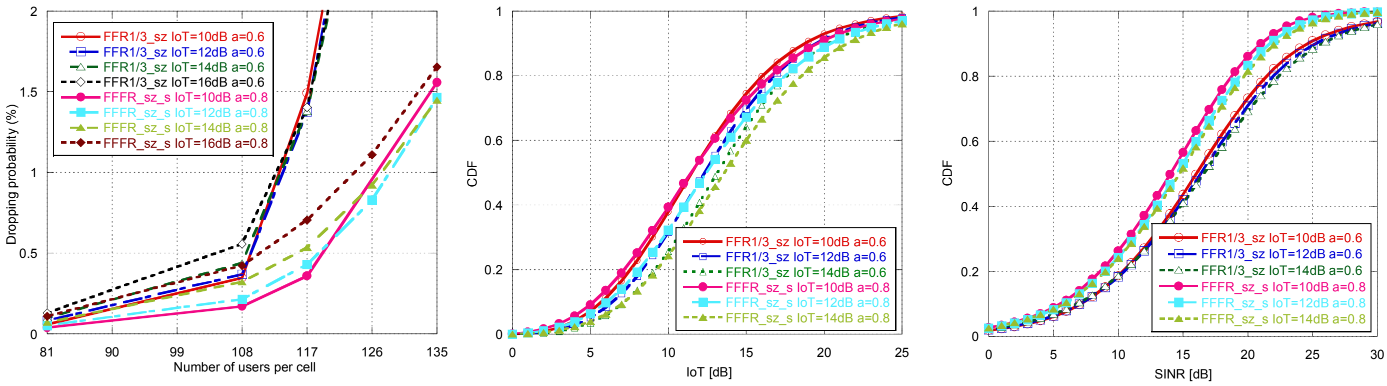

a) Dropping Probability b) CDF global IoT (108 UEs per cell) c) CDF global SINR(108 UEs per cell)

Figure 4. Dependence of the system performance with IoT_{OBJ}

V. CONCLUSION

In this paper, we have studied the dependence between FPC and different ICIC/ISIC schemes in an SC-FDMA multi-cell system. Our study reveals that, in order to increase the cellular system performance, a different FPC operation point must be set depending on the per-cell or per-sector basis of the frequency reuse strategy being considered in the interference coordination scheme. In particular, a higher value must be set for α when frequency resources are reused on a per-sector basis. Our results suggest a value of α=0.6 when frequency resources are reused only once per cell, and a value of α=0.8 if frequency resources are reused on a per-sector basis.

ACKNOWLEDGMENT

This work has been supported by the Spanish Government through the grant TEC2011-23037 from the Ministerio de Ciencia e Innovación (MICINN).

REFERENCES

[1] 3GPP, TS 36.211, v8.5.0 "Physical Channels and Modulation", 2008.

[2] L.Liu, J.Zhu, X.Tao, Y.Wang, P.Zhang "A novel scheme for OFDMA based E-UTRA uplink", Proc. IEEE Wireless Communications and Networking Conference (WCNC) 2007, pp.1373-1377.

[3] B. Rengarajan, A.L. Stolyar, H. Viswanathan, "Self-organizing Dynamic Fractional Frequency Reuse on the uplink of OFDMA systems", Proc. 44th Annual Conference on Information Sciences and Systems (CISS), 2010, pp. 1–6.

[4] M.Porjazoski, B.Popovski, "Impact of Fractional Frequency Reuse on LTE Performances in Uplink", Proc. 26th IEEE Convention of Electrical and Electronics Engineers in Israel, 2010, pp.81-85.

[5] 3GPP TS 36.213, v8.5.0 "Physical Layer Procedures", 2008.

[6] A.Simonsson, A.Furuskar, "Uplink Power Control in LTE: Overview and Performance", Proc. 68th IEEE Vehicular Technology Conference (VTC), 2008- fall, pp.1-5.

[7] B.Muhammad, A.Mohammed, "Performance Evaluation of Uplink Closed Loop Power Control for LTE System ", Proc. 70th IEEE Vehicular Technology Conf. (VTC), 2009- fall, pp.1-5.

[8] M.Boussif, N.Quintero, F.D.Calabrese, C.Rosa, J.Wigard, "Interference Based Power Control Performance in LTE uplink", Proc. Int. Symp. on Wireless Communications Systems 2008 (ISWCS`08), pp.698-702.

[9] Y.Xang, J.Luo, C.Hartmann, "Inter-cell interference mitigation through flexible resource reuse in OFDMA based communication networks". Proc. European Wireless, 2007

[10] I.Guío. A.Hernández, J.Chóliz, V.Montero, J.Lafuente, A.Valdovinos, "Radio resource management in OFDMA systems for strong frequency reuse in sectorized deployments". Proc. 7th International Symposium on Wireless Communications Systems 2010 (ISWCS'10), pp.641-645.

[11] 3GPP, TSG RAN WG1#51 R1-074850, "Uplink power control for E_UTRA – range and representation of P_O ", Ericsson, Nov. 2007.

[12] J.Lafuente, A.Hernández, A Valdovinos, "Sector-Based Radio Resource Management for SC-FDMA Cellular Systems", Proc. 8th Int. Symp. on Wireless Communications Systems 2011 (ISWCS'11), pp.750-754.

[13] C.Úbeda, D.López, C.Rosa, K.L.Pedersen, F.D.Calabrese, P.H. Michaelsen, J.Michel, "Performance of Uplink Fractional Power Control in UTRAN LTE", Proc. 69th IEEE Vehicular Technology Conf. (VTC) 2008-Spring. pp. 2517-2521.